Journal of Hydrology 502 (2013) 37–52

Contents lists available at ScienceDirect

Journal of Hydrology

journal homepage: www.elsevier.com/locate/jhydrol

The impacts of climate change and land cover/use transition on the hydrology in the upper Yellow River Basin, China

Lan Cuo [a,*], Yongxin Zhang [b], Yanhong Gao [c], Zhenchun Hao [d], Luosang Cairang [e]

[a] Key Laboratory of Tibetan Environment Changes and Land Surface Processes, Institute of Tibetan Plateau Research, Chinese Academy of Sciences, Beijing, China
[b] Research Applications Laboratory, National Center for Atmospheric Research, Boulder, CO, United States
[c] Key Laboratory of Land Surface Process and Climate Change in Cold and Arid Regions, Cold and Arid Regions Environmental and Engineering Research Institute, Chinese Academy of Sciences, Lanzhou, Gansu Province, China
[d] State Key Laboratory of Hydrology-Water Resources and Hydraulic Engineering, Hohai University, Nanjing, Jiangsu Province, China
[e] Qinghai Agriculture and Forestry Administration, Xining, Qinghai Province, China

ARTICLE INFO

Article history:
Received 2 April 2013
Received in revised form 10 July 2013
Accepted 3 August 2013
Available online 9 August 2013
This manuscript was handled by Konstantine P. Georgakakos, Editor-in-Chief, with the assistance of Daqing Yang, Associate Editor

Keywords:
Hydrological processes
Hydrological modeling
Climate change and land cover change/use impacts
The upper Yellow River Basin

SUMMARY

Observed streamflow over the past decades in the upper Yellow River Basin (UYRB) was examined for changes in hydrological regime. The modified Variable Infiltration Capacity (VIC) model was employed to better understand climate change impact and long-term and recent land cover/use change impact as it relates to the "Grain for Green Project" and "Three Rivers Source Region Reserve" on water resources by examining mechanisms behind observed streamflow changes.

UYRB hydrological regimes have undergone changes over the past decades as reflected by a decrease in wet and warm season streamflow, and annual streamflow. Progressively more streamflow has been generated in the early part of the year compared to the latter part, consequently leading to the earlier occurrence of the day representing the midpoint of yearly mass flow. VIC simulations suggest that these changes in observed streamflow were due to the combined effects of changes in precipitation, evapotranspiration, rainfall runoff, and baseflow and were caused primarily by climate change above Tang Nai Hai (TNH) hydrometric station. Below TNH where human activity is relative intense, land cover/use change and reservoir release impacts became important. Changes in snowmelt runoff were negligible over the past decades. Owing to this, snowmelt runoff appeared to play only a modest role in the changing hydrology of the region. The conservation programs were shown to start to exhibit some positive impacts on water resources in the UYRB.

1. Introduction

The Yellow River, considered the cradle of Chinese civilization, originates in northern Tibetan Plateau (TP), flows through the Loess Plateau and the North China Plain, eventually empties into the Bohai Sea to the east of China. It supports 30% of China's population (Huang et al., 2009) and 13% of China's total cultivated area (Cai and Rosegrant, 2004). The Yellow River's headwater is situated in the Bayan Har mountain range in southern Qinghai Province of northern Tibetan Plateau (Fig. 1). The upper Yellow River Basin (UYRB) above the Tang Nai Hai (TNH) hydrometric station contributes approximately 35% of the total annual discharge in disproportion to its 15% area of the entire Yellow River Basin (Hu et al., 2011). Fragile and unique temperate, alpine, and wetland ecosystems within the UYRB rely on its available water resources. Understanding UYRB hydrological processes, especially in the context of global climate change and increased human activity, is necessary for informed current and future sustainable management of its water resources. Streamflow, being an integrated component of hydrology in a basin, and changes in streamflow reflect the combined effects of climate, vegetation, and soil (Rodriguez-Iturbe et al., 2001). It is important to understand how climate, land cover/use change will impact streamflow and, hence, available water resources on a basin scale.

A number of observational studies have shown that streamflow measured at TNH decreased over the past decades (Cao et al., 2006; Tang et al., 2008; Hu et al., 2011). Cao et al. (2006) found that TNH annual discharge exhibited a statistically non-significant decreasing trend between 1956 and 2000. Seasonally, except for increases detected for April, May, and June, all other months exhibited decreases in discharge. Hu et al. (2011), who analyzed TNH streamflow for a prolonged period of time (1959–2008), found that decreasing TNH streamflow was associated with decreasing wet season (from May to September) precipitation and rising temperatures. The same authors speculated that the source region

* Corresponding author. Address: Building 3, Courtyard 16, Lincui Road, Chaoyang District, Beijing 100101, China. Tel.: +86 010 84097091; fax: +86 010 84097079.
E-mail address: lancuo@itpcas.ac.cn (L. Cuo).

0022-1694/$ - see front matter
http://dx.doi.org/10.1016/j.jhydrol.2013.08.003

catchment was largely undisturbed by human activity, which led the authors to conclude that decreasing streamflow was predominantly caused by climate change. Most of these studies focused on the revelation of the changes based on the correlation analysis between streamflow and temperature/precipitation, whereas the mechanisms that link climate change to streamflow change were rarely explored. Also, few studies examined streamflow changes at hydrometric stations other than TNH in the UYRB and it is unclear whether or not their findings are applicable to the entire UYRB.

Like elsewhere on Earth, climate change is taking place in the Yellow River Basin as reported by Wang et al. (2001), Fu et al. (2004), Yang et al. (2004), Xu et al. (2007), Zhao et al. (2007), Tang et al. (2008), Zhang et al. (2008) and Hu et al. (2011). These studies consistently describe basin-wide temperature increases, tempo-spatial variations in precipitation changes, and decreases in water resources in the Yellow River Basin. Based primarily on statistical trend analyses of observed climatology, many of these studies speculated that changes in water resources have resulted from climate change, especially changes in precipitation and temperature. What are lacking in these studies are in-depth analyses and the quantification of the changes in water balance terms related to climate change.

Snow has been widely recognized as an important component of water resources in cold regions. As suggested by Barnett et al. (2005) and Stewart (2009), snowpack changes in a warming climate were altering hydrological cycles and water availability. Clearly, the validity of this assertion relies on several factors, such as the proportion of snow to total precipitation, seasonal cycles of storm occurrences, elevation, and air temperature. As an example, in the Pacific Northwest (PNW) of the United States of America where major storm systems occur in winter and where winter average air temperature is around 0.5 °C (Mote and Salathe, 2010; Gao et al., 2011), rising temperatures in the past have greatly affected winter snow–rain partitioning (Hamlet et al., 2005), resulting in a transition from nival to pluvial hydrological regimes for low to midrange elevation basins (Cuo et al., 2009). Similar transitions are also projected for PNW highland basins in the mid-21st century as global warming progresses (Cuo et al., 2011).

To date, there has been limited research but with mixed reports concerning the role of snow in UYRB hydrology as well as the impacts of snow change on UYRB streamflow. Lan et al. (1999) reported on the importance of snowmelt in the UYRB, especially during springtime when snowmelt accounts for nearly 40% of total runoff. However, Immerzeel et al. (2010) found that during 2000–2007 meltwater derived from snow and ice played only a modest role in mean annual streamflow across the upstream region of the Yellow River Basin (elevation greater than 2000 m). To what degree snowmelt contributes to UYRB water resources certainly merits further investigation.

Besides climate change, human activity (e.g., agriculture, industrialization, urbanization, ecosystem conservation and reservoir operation) induced land cover/use change also influences UYRB water resources and hydrology. This appears to be especially true considering that human intrusion within this particularly harsh but pristine environment has increased in recent decades. As an example, Li and Liu (2004) and Dong et al. (2005) reported widespread grassland degradation in the UYRB during the 1980s and the 1990s and attributed the degradation to intensification of human activity such as overgrazing and digging caterpillar fungus. The recognition of human disturbance to the local ecosystem led to the implementation of the "Grain for Green Project" (GGP) ecosystem restoration initiative in 2000. The GGP was aimed at turning the previously cultivated and grazed land back into forests and pastures by providing subsidies to farmers and nomads in the form of grain and cash. Later, in 2005, Qinghai provincial and China central governments also launched an eco-environmental protection project and established the Three Rivers Source Region Reserve (TRSRR), comprised of the headwaters of the Yellow River, the Yangtze River, and the Mekong River that lie side by side in southern Qinghai Province. These efforts represent intensive human intervention aimed to ameliorate ecosystem degradation. However, it is unknown to what extent the intensive intervention has influenced water resources in the region and whether or not the intervention has been effective.

A few studies have examined the impacts of both climate change and land cover/use change on UYRB hydrology. For example, Zhao et al. (2009) used sensitivity-based analysis and a dynamic water balance model to study the impacts of climate change as manifested by precipitation and potential evapotranspiration (ET) change and the impacts of vegetation change, respectively, on streamflow at the Jimai, Tang Nai Hai, and Lan Zhou hydrometric stations in the UYRB in 1956–2000. Their results showed that vegetation change played a secondary role in affecting changes in streamflow at Tang Nai Hai while both climate change and vegetation change were important factors at Lan Zhou. On the other hand, Zheng et al. (2009) applied the concept of climate elasticity to assess the impacts of climate and land surface changes on UYRB streamflow from 1960 to 2000, and showed that land use changes played a more important role in reducing streamflow during the 1990s. Apparently, the inconsistencies between these studies stem from the different methods, time periods, and base scenarios used. None of these studies examined the influence of the recent large-scale human intervention on streamflow in the region.

This study, by applying a rigorously calibrated and validated physically-based macroscale hydrological model over the UYRB, aims to identify changes in observed streamflow at several locations and to explore the causes of streamflow changes by examining climate change impacts on water balance terms, and land cover/use change (both long term and recent human intervention) impacts on streamflow. Furthermore, this study tries to reveal the importance of snowmelt contribution to streamflow. The ultimate objective of this study is to identify the mechanisms that are responsible for streamflow changes in the UYRB.

2. Study area

The UYRB, situated above Jingyuan County, Gansu Province (JYR, 36°45′N, 104°45′E, 1400 m above mean sea level), is the area investigated in this study (Fig. 1). Previous studies focused mainly on the Yellow River Basin above TNH (headwater region) where population density is low (6/km^2 based on the 2003 census data). This study also includes areas below TNH and above JYR where two economic centers, Xining City and Lanzhou (LZH) City are located. In total, about 5.8 million people live in the Xining and Lanzhou corridor.

According to a 90-m elevation map, UYRB elevation ranges between 1400 m and 6300 m and drops off from the southwest to the northeast. TNH hydrometric station (35°30′N, 100°9′E, 2700 m) is located just above the Longyang Gorge Reservoir (247×10^8 m^3 water storage capacity) in Qinghai Province. Ji Mai (JMA, 33°46′N, 99°39′E, 3955 m), Tang Ke (TAK, 33°25′N, 102°28′E, 3435 m), and Ma Qu (MAQ, 33°58′N, 102°5′E, 3435 m) hydrometric stations are located upstream of TNH. Streamflow measured at and above TNH had not been affected by large dams or major irrigation diversions and as a result largely reflected the natural conditions. Near JYR, LZH gauge (36°04′N, 103°49′E, 1600 m) is located, and right above LZH, there is another large reservoir, the Liujia Gorge Reservoir (64×10^8 m^3 water storage capacity). Both reservoirs could be expected to affect streamflow at LZH. Also, below the

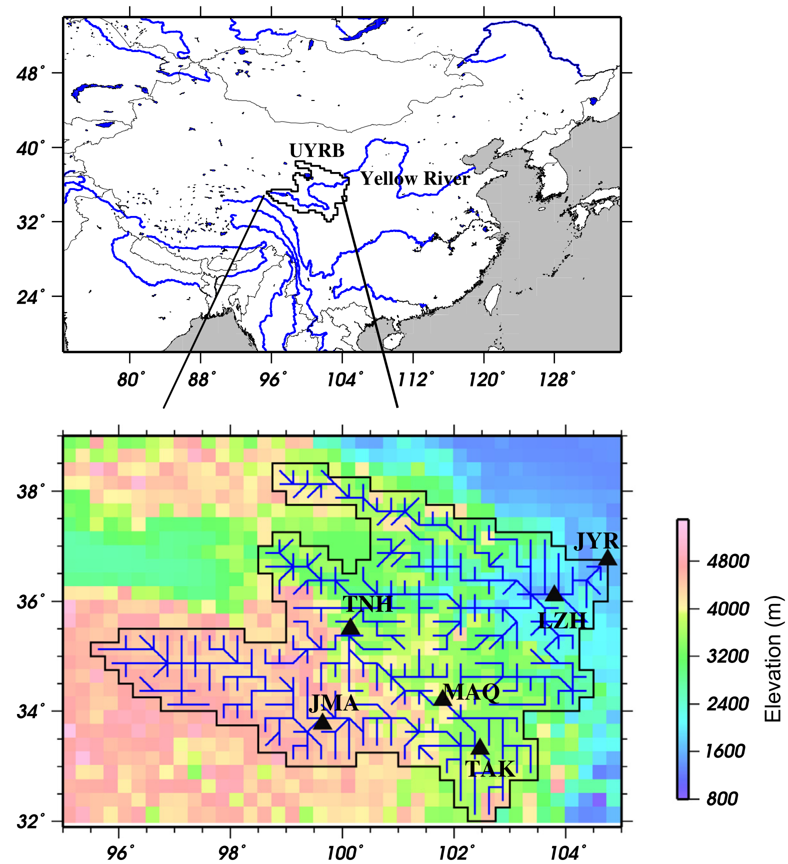

Fig. 1. Location and elevation of the upper Yellow River Basin. Major rivers originating from the Tibetan Plateau are displayed in the top panel. Blue lines in the bottom panel represent the Yellow River channels, and black lines outline the upper Yellow River Basin. Triangles inside the basin denote the Ji Mai station (JMA), Tang Ke station (TAK), Ma Qu station (MAQ), and Tang Nai Hai station (TNH) in Qinghai Province, and Lan Zhou station (LZH) in Gansu Province. Triangle in the northeast of the basin represents the outlet of the upper Yellow River Basin in Jing Yuan County, Gansu Province (JYR).

Longyang Gorge Reservoir, human activity, such as agriculture, industry and urbanization, is relatively intense and land cover/use changes are inevitable. Areas of contribution for JYR, LZH, TNH, MAQ, TAK, and JMA are approximately 240,000 km^2, 220,000 km^2, 122,000 km^2, 109,000 km^2, 7800 km^2, and 57,000 km^2, respectively.

The entire UYRB is situated within a semiarid region with an approximate total annual precipitation of 500 mm and an approximate mean annual air temperature of 0.7 °C. Large-scale atmospheric systems that affect UYRB weather and climate are the subtropical westerly jet stream, the El Niño-Southern Oscillation (ENSO), the North Atlantic Oscillation (NAO), and the Arctic Oscillation (AO) in winter and ENSO, the subtropical westerly jet stream, the East Asian summer monsoon, and the South Asian summer monsoon in summer (Cuo et al., 2013).

UYRB land cover is dominated by temperate and alpine grasslands and alpine meadows (Zhou et al., 1987). The geological feature of the study area is principally characterized by Triassic flysche sandstone. In general, UYRB soil is poorly developed and relatively young in its overall lifespan. Sand is the main component of soil texture in the region (FAO, 2008). Fine, medium, and coarse gravel are also common to this region. Soil textures in the top 1 m are primarily sandy loam in the west and loam in the east (FAO, 2008).

3. The Variable Infiltration Capacity (VIC) model

The Variable Infiltration Capacity model (VIC, Liang et al., 1994, 1996) was employed for this study to investigate and understand the impacts of climate change and land cover transition on UYRB hydrology. VIC is a physically-based macroscale hydrological model developed to solve water and energy balances. It has been applied in many parts of the world in a range of climate conditions and resolutions (Abdulla and Lettenmaier, 1997; Lohmann et al., 1998b; Matheussen et al., 2000; Durre et al., 2000; Nijssen et al., 2001; Rhoads et al., 2001; Christensen et al., 2004; Haddeland et al., 2006; Adam et al., 2007). VIC has been demonstrated to perform especially well in simulating streamflow in humid environments (Abdulla and Lettenmaier, 1997). One of its appealing features relevant to the current study is its capacity to simulate cold region hydrology by incorporating mechanisms of frozen soil and snow accumulation and ablation (Cherkauer and Lettenmaier, 1999, 2003).

The infiltration rate for VIC is specified as a power function of the maximum infiltration capacity and basin saturation area, and is controlled by an empirical parameter (Zhao et al., 1980). Hence, changes in the infiltration rate result in soil moisture spatial variability. For VIC, baseflow responds both linearly and nonlinearly to soil moisture changes depending on bottom layer soil moisture conditions and flow rates, which is realized using the empirical Arno model conceptualization (Todini, 1996). VIC solves both energy and water balances for individual cells of a grid that represents a watershed. The streamflow routing model developed by Lohmann et al. (1998a) can be launched after VIC concludes energy and water balance calculations for a watershed. Input data for VIC include meteorological forcing data (temperature minima and maxima, wind speed, precipitation), vegetation and soil characteristic parameters. For this study, a modified version of VIC (v4.1.1) that also takes into account UYRB irrigation practices as well as the differentiation between snowmelt and rainfall surface runoff was used to investigate hydrological dynamics of this particular region.

Land cover and land use are represented by land cover/use class IDs, areal fractions, vegetation root zone depths, and root zone fractions of individual cells. Other land cover parameters involved in water and energy balances such as monthly leaf area index (LAI), albedo and stomatal resistance are specified for each land cover/use class and referenced by class IDs. When irrigated cropland is present within a cell, the irrigation timing (at a monthly time step) and the amount of water required are also listed for the cell. Land cover/use classes, areal fractions of classes, root zone and other characteristics involved in the energy and water balances for certain locations represented by grid cells will be different under different land cover scenarios. Such differences will cause different hydrological processes in areas of interest, which can be simulated by VIC.

In the northern Tibetan Plateau region, irrigation is not a major agricultural practice. This is especially true throughout Qinghai Province where 80% of the UYRB is situated, for which approximately only one-third of the total agricultural land ($\sim$5333 km^2) is irrigated. Nevertheless, the effect of irrigation on hydrological processes needs to be considered in view of the GGP and other conservation projects. For this study, irrigation and its effects are accounted for in VIC through the modifications discussed below.

According to Qinghai Local Disaster Classifications (Government Document ID: DB63), when soil moising to Qinghai Local Disaster Classifications (Government Document ID: DB63), when soil moisture is reduced to 60% below field capacity, the soil is considered to be under a drought condition and irrigation is required. Irrigation in the UYRB usually takes place during the months of February, March, and June. To model irrigation, a scheme was developed that combines irrigation timing, surface runoff, and soil moisture redistribution, depending on the ratio of soil moisture to field capacity. Specifically, during the irrigation months, a comparison is first made between the previous 10 day averaged top root zone soil moisture or accumulated 10 day precipitation and 60% field capacity in the top root zone for grid cells that contain irrigated cropland. If the 10 day averaged soil moisture or totalprecipitation is less than 60% of field capacity, the amount of water equivalent to 60% of field capacity is extracted from surface runoff (that would have been routed to stream channels) and is added to the top root zone soil moisture. The added top zone soil water content would then be fully involved in the processes of soil evaporation, runoff generation, and root zone soil water flux. The remaining surface runoff would subsequently be routed to the stream channel. Note that the 60% threshold and the irrigation months are set as input parameters and therefore can be conveniently adjusted if required.

Distinguishing between snowmelt runoff and rainfall runoff was based on the model simulated rainfall, snowmelt, soil moisture, and surface runoff in a time step. For example, if both snowmelt and runoff take place in a time step where no rainfall is present, surface runoff would then be considered as snowmelt runoff only. If snowmelt and rainfall both take place in a time step, surface runoff would then be adjusted by the ratio of snowmelt inflow to the total soil moisture from which total surface runoff is generated. If no snowmelt is present, runoff would be produced by rainfall only.

4. Data

4.1. Forcing data and streamflow

This study used a gridded historical dataset at 0.25° $\times$ 0.25° resolution generated for northern Tibetan Plateau (Cuo et al., 2013) to drive VIC simulations. The dataset contains daily precipitation, 2 m temperature maxima and minima, and 10 m wind speed from 1957 to 2009. Gridded data were created from observations taken from 81 meteorological stations situated within northern Tibetan Plateau using the Synographic Mapping System (SYMAP, Shepard, 1984) and elevation-based gridding processes to account for changes in temperature, wind speed, and warm and wet season precipitation over varying elevations (Cuo et al., 2013). Station observations were obtained from the China Meteorological Administration and the Qinghai Institute of Meteorology and were fully quality controlled.

In order to examine the impacts of climate change on UYRB water resources, two sets of climate forcing data representing the climate conditions for the beginning and ending periods of 1957–2009 were generated using the gridded data. These two sets of data were referred to as "climate 1957" and "climate 2009," respectively, and were created as follows: first, the linear monthly trends in precipitation, temperature maxima and minima, and wind speed were calculated for the period between 1957 and 2009 in each grid cell; second, the pivotal year 1957 (or 2009) was chosen as the baseline upon which the trends were removed from (or added to) the daily time series in each grid cell using a linear relationship to generate climate 1957 (or 2009). The inter- and intra-annual variability of the historical climate records was thus preserved in climate 1957 and climate 2009 since both datasets were constructed through perturbing the original daily time series with the linear trends.

For the historical climate records, the trends of temperature maxima and minima, and wind speed were statistically significant ($\alpha = 0.05$) across the UYRB (Cuo et al., 2013). Precipitation exhibited statistically significant trends in eastern and northwestern UYRB (Cuo et al., 2013). The construction of climate 1957 and 2009 was conducted in every grid cell covering the UYRB, hence the observed spatial variability of climate change was preserved.

Daily streamflow data for JMA (1959–2009), TAK (1981–2009), MAQ (1960–2009), TNH (1956–2009), and LZH (daily: 1956–1997; monthly: 1956–2000) were obtained from the Hydrological Bureau of the Ministry of Water Resources of China. TNH measurements were used to calibrate VIC while model validation was carried out at JMA, TAK, MAQ and TNH. The choice of TNH as the calibration site was because of (a) the comparatively little human activity that took place upstream of TNH, (b) the longest available streamflow measurement record, and (c) the largest area coverage suitable for macro-scale modeling.

To examine the reservoir impacts on streamflow in the UYRB, we used monthly inflow and outflow of Longyang Gorge and Liujia Gorge measured at four gauges. For Longyang Gorge, the inflow gauge is Tang Nai Hai (TNH, details see above) and the outflow gauge is Gui De (GDE, 36°02′N, 101°24′E, contribution area 133,650 km^2), and the analysis began from 1986 when the operation started. For Liujia Gorge, the inflow gauge is Xun Hua (XHU, 35°50′N, 102°30′E, contribution area 177,275 km^2) and the outflow gauge is Xiao Chuan (XCH, 35°56′N, 103°20′E, contribution area 181,770 km^2), and the analysis began from 1968 when it was operated. At both dams, the available inflow and outflow data ended in 2002.

4.2. Vegetation and soil data

For this study, VIC vegetation and soil parameters are adopted from ftp://ftp.hydro.washington.edu/pub/HYDRO/models/VIC/Veg/veg_lib and http://www.hydro.washington.edu/Lettenmaier/Models/VIC/Documentation/SoilParam.shtml, respectively. Soil textures are obtained from FAO (2008).

The land cover map for 1994 (hereafter referred to as "land cover 1994") was downloaded from http://www.glcf.umd.edu/data/

landcover/. This global land cover classification dataset was compiled in 1998 using imagery from the Advanced Very High Resolution Radiometer (AVHRR) satellites acquired between 1981 and 1994 (Hansen et al., 2000). Evaluations of the land cover data using field measurements obtained by the United States of America and European food and agricultural agencies have shown to be of good quality throughout most parts of the world except for Africa where the data quality appears to be relatively inferior (Hansen et al., 2000).

Since reliable land cover data during the late 1950s and the early 1960s do not exist, we constructed land cover 1960s using land cover 1994 based on previous findings that the major land cover change in the UYRB and the surroundings between the 1960s and the 1990s has been grassland degradation (Chen and Liu, 2007; Dong et al., 2005; Li and Liu, 2004; Fu et al., 2007). The construction of land cover 1960s involved several steps. First, the population of the UYRB was obtained for 1964 and 1994 based on census data from the China National Bureau of Statistics for 1964, 1990 and 2000 (http://www.stats.gov.cn/tjgb/rkpcgb). Second, the population ratio between 1964 and 1994 (there were no 1994 census data and we used the average of 1990 and 2000 census data as a proxy) was computed and a scaling factor was obtained by one minus the population ratio (1/2). Third, the peripheral areas of all land cover types except for grassland and forest in land cover 1994 were converted to grassland and the converted areal coverages were about 50% of the original coverages assuming that the scaling factor 1/2 was an indication of 50% land cover/use change resulted from population change. The converted land is less than 10% of the whole UYRB area.

For this study, cropland was divided into irrigated and non-irrigated cropland using an elevation threshold of 2700 m. This was based on the fact that irrigated cropland is usually distributed along river banks in the UYRB where elevation is lower than 2700 m. Table 1 provides land cover types, percentage coverage, and cell numbers of each classification over the study area for land cover 1994. Dominant UYRB land cover types are grassland and shrubland (Table 1), followed by cropland and woodland.

5. Analysis

Long-term Mann–Kendall trends in monthly and annual streamflow, monthly to annual flow ratios, and day representing the midpoint of yearly mass flow were examined to detect changes in observed streamflow over the past decades. The monthly to annual flow ratio and day representing the midpoint of yearly mass flow, computed following Stewart et al. (2005), represented contributions of monthly flow to the annual total and the overall distribution of flow during a 1-year period, respectively. The mechanisms that caused streamflow changes were explored through the examination of VIC simulated water balance terms under two climate scenarios (climate 1957 and 2009) and streamflow for two land cover scenarios (land cover 1960s and 1994).

Historical daily meteorological forcing data and land cover 1994 were used during calibration. VIC was calibrated using daily TNH streamflow measurements from 1987 to 1997. Daily and monthly streamflow measurements at JMA, TAK, MAQ, and TNH were also used to validate VIC. Snow cover estimates from satellites were used to evaluate VIC simulated snow cover.

The delta approach was utilized for examining the responses of water balances to changes in temperature, precipitation and wind speed to better understand climate change impact. Delta values were the monthly mean changes in each variable between climate 2009 and 1957 and represented the average climate trends in the basin in 1957–2009. For example, to examine temperature sensitivity, the averaged changes in monthly temperature between climate 2009 and 1957 were added to the daily temperature time series in climate 1957, while keeping precipitation and wind speed unchanged in climate 1957. Likewise, precipitation and wind speed were perturbed in the same way. Because the mean monthly trends of temperature, wind speed and precipitation were used to perturb the daily time series, the inter-annual and intra-annual climate variability of the original time series were preserved. The response of water balance terms to changes in temperature, precipitation and wind speed can then be obtained by investigating the differences in water balance terms between the perturbed and the control (unperturbed) runs.

More than 50 year climate records were used to study climate change impacts on hydrology. When climate gradually changes over a long period of time, the beginning and ending conditions could represent the beginning and ending status of the changes. For this study, the beginning (1957) and the ending (2009) climate records were chosen to represent historical and current climate conditions, respectively. Two simulations were subsequently carried out using climate 1957 and climate 2009 alongside land cover 1994 as a way to isolate impacts of climate change on water balances and streamflow.

Land cover/use change can be caused by human activity and climate change. In this study, land cover/use change is a broad term that includes climate change induced and human activity such as agriculture, industry, urbanization and ecosystem conservation induced ground surface changes. In the UYRB, precipitation and temperature changes can affect vegetation growth, but they may not be able to cause dramatic plant succession changes in the 50-year study period. Only human activity can result in the conversions between different land cover types in a short period of time that are important to consider from the water resources perspective. As a physically-based hydrological model, VIC takes into accounts the seasonal variations in LAI, albedo and other vegetation parameters. However, VIC is not able to simulate vegetation succession, nor does it consider urban water usage and reservoir operations. On the other hand, dramatic land cover change primarily caused by human activity can be realized in the model through changing vegetation types. By comparing simulated and observed streamflow, we are able to show the impacts of land cover change as a whole.

Land cover 1960s and 1994 were used to study long term and recent land cover/use change impacts on streamflow. Recent land cover/use change was assumed to be the result of the GGP and TRSRR implemented in Qinghai Province. To isolate long term and recent land cover change effects from climate change effects, two simulations were conducted using land cover 1960s and land cover 1994 driven by historical climate records. Both simulations were compared to observations for the same time period, i.e., simulations using land cover 1960s (1994) were compared to

Table 1
Land cover types, areal percentage and cell numbers for land cover 1994 in the upper Yellow River Basin.

Land cover (ID)	1994
Percent coverage (%) (cell numbers)	
Water (0)	1.22 (5219)
Evergreen needle leaf (1)	2.40 (10,264)
Deciduous broad leaf (4)	0.18 (777)
Mixed forest (5)	0.54 (2311)
Woodland (6)	6.85 (29,342)
Wooded grassland (7)	14.79 (63,362)
Closed shrubland (8)	2.15 (9225)
Open shrubland (9)	16.72 (71,626)
Grassland (10)	45.72 (195,855)
Non-irrigated cropland (11)	6.11 (26,160)
Irrigated cropland (20)	2.10 (8986)
Bare ground (12)	1.18 (5057)
Urban and built (13)	0.05 (216)

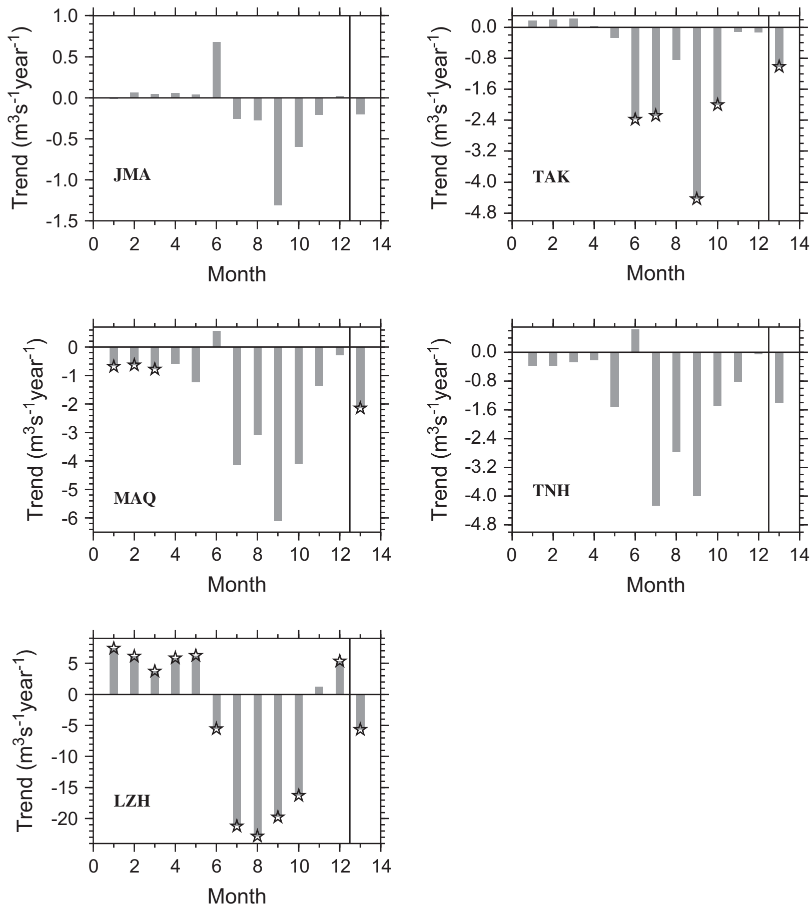

Fig. 2. Trends in the observed monthly and annual streamflow at JMA (1959–2009), TAK (1981–2009), MAQ (1960–2009), TNH (1956–2009), and LZH (1956–2000). Stars represent statistically significant trends at $p < 0.1$.

streamflow observations beginning in 1960 (1994). It was assumed that observed streamflow reflects the influence from both climate and land cover/use change, and the simulations with fixed land cover only contain the climate change impacts. The residuals between the observations and the simulations represent the isolated land cover/use change impacts for the study period (Bowling et al., 2000; Cuo et al., 2009). Here, only streamflow was examined in the analysis as other water balance terms were not observed.

Inflow, outflow and contribution areas were used to analyze the reservoir impacts. The increase in the contribution area from the inflow gauge to the outflow gauge was used to scale the annual inflow. The scaled inflow was the estimation of annual natural flow at the outflow gauge. The relative difference between estimated and observed mean annual flow at the outflow gauge then reflected the impacts of the reservoir.

6. Results

6.1. Trends in observed streamflow

Trends in observed streamflow for all five stations are provided in Fig. 2. Most monthly trends were negative above TNH, with statistically significant negative trends were found in June, July, September, and October for TAK and January through March for MAQ. Compared to the other months, JMA, TAK, MAQ and TNH experienced noticeably large negative trends between July and October, although these trends were not statistically significant except for TAK. Relatively large but statistically insignificant positive trends were noted only in June for JMA, MAQ, and TNH. LZH experienced significantly negative trends in June–October. From December through May, however, statistically significant positive trends were noted for LZH, which was not the case at the other stations. All stations reported negative annual trends, and they are statistically significant at TAK, MAQ and LZH (Fig. 2).

The monthly to annual streamflow ratio (Fig. 3) showed small trends that to a large extent followed patterns of monthly streamflow for all stations. Negative trends primarily occurred between July and October, with September exhibiting the largest or nearly the largest trends for all stations (statistically significant at TAK and LZH). Positive trends predominantly occurred during the dry season between November and June (with most statistically significant trends noted for TAK and LZH). June corresponded to the largest positive trends for all stations except TAK where a small negative trend was detected (Fig. 3). Such distributions in ratios appear to suggest that despite negative trends in monthly streamflow at most stations as shown in Fig. 2, positive contribution to annual streamflow have been progressively on the rise in the early part (compared to the middle part). This is also consistent with decreasing trends for days representing the midpoint of observed mass flow (which occurred progressively earlier) for all five stations (lower right panel in Fig. 3), possibly indicating changes in the UYRB hydrological regime.

6.2. Calibration and validation of VIC

Fig. 4 provides observed and VIC simulated daily and monthly streamflow for 1987–1997 (calibration period so as to cover the

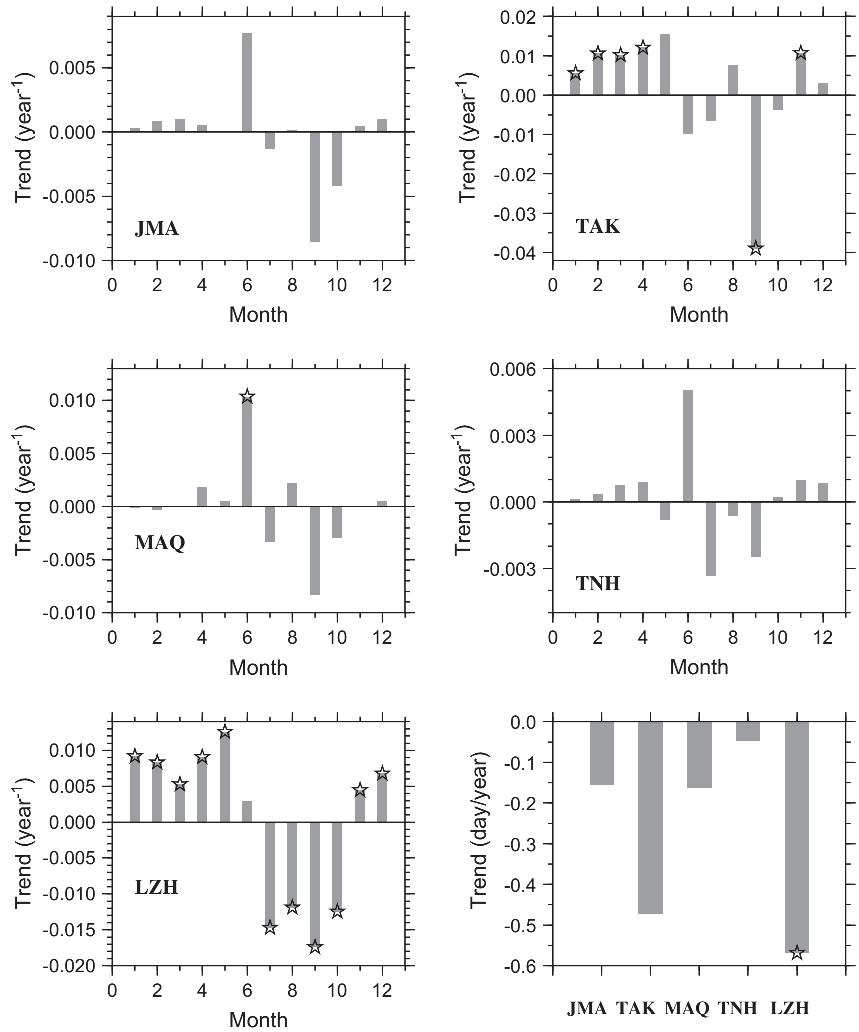

Fig. 3. Trends in the ratio of the observed monthly to annual flow at JMA, TAK, MAQ, TNH and LZH, and trends in the center days of the observed yearly mass flow at the 5 stations (lower right panel). Stars represent statistically significant trends at $p < 0.05$.

1994 land cover period) and for 1977–1987 (validation period) for TNH (statistics provided in Table 2). Simulations during the calibration period captured the observed evolution and magnitude reasonably well for both daily and monthly time scales. Rising limbs of daily hydrographs and baseflow were simulated especially well. Both observations and simulations also exhibited generally decreasing trends in TNH streamflow between 1987 and 1997. Deficiencies in VIC simulations included overestimation of descending limbs for 1990, 1992, 1994, 1995, and 1997, and mismatched peak flows for 1989, 1992, 1993, 1995, and 1997, which was most likely due to errors in extreme precipitation in the forcing data. During the calibration period, mean model bias was 4% for both daily and monthly streamflow (Table 2). Correlation coefficients (R), root mean square errors (RMSE), and Nash–Sutcliffe (NS) coefficients for daily series in the calibration period were 0.86, 246.1 $m^3 s^{-1}$, and 0.74, respectively. At a monthly time step, statistics were slightly improved (Table 2). Table 3 lists calibrated parametersand their values.

During the validation period, rising limbs and baseflow were also simulated well (Fig. 4). Peak flow simulations improved during the validation period in comparison to the calibration period. Mean model bias was −1% for both daily and monthly time series, and R, RMSE, and NS coefficients were 0.89, 295.5 $m^3 s^{-1}$, and 0.80, respectively, for daily streamflow (Table 2). The slightly better statistical values for monthly streamflow were due to the smoothing out of daily variability.

Model statistics were reasonably satisfactory for JMA, TAK, and MAQ throughout the validation period considering that VIC was not calibrated specifically for these stations (Table 2). For JMA and TAK, capturing streamflow from smaller sub-basins (see Fig. 1), simulated streamflow exhibited the lowest NS among all stations. This was likely due to the coarse resolution (0.25° by 0.25) represented by VIC. On the other hand, the model captured temporal variability of observed streamflow for JMA and TAK reasonably well as reflected by the high R in excess of 0.68 for both daily and monthly time series. For MAQ, the model exhibited rather similar statistics to those for TNH (Table 2). The good performance of VIC at MAQ and TNH implies that the model in its current settings can be used to study streamflow in un-gauged basins of similar physical properties.

In order to evaluate the performance of VIC in simulating snow, MODIS snow cover data (MODIS/Terra Snow Cover L3 monthly 0.05 degree Grid MYD10CM) for 2003–2009 and Northern Hemisphere 25-km EASE-Grid Weekly Snow Cover and Sea Ice Extent Version 3 data for 1972–2006 (Armstrong and Brodzik, 2005) were used. The intention of using both EASE-Grid and MODIS snow measurements was to not only include as many sources of snow data as possible but also to extend the period of UYRB snow cover estimation so that long-term VIC simulations could be evaluated. Fig. 5 provides satellite estimated and VIC simulated mean annual and monthly snow cover for the area above JYR. Agreement between MODIS estimated and VIC

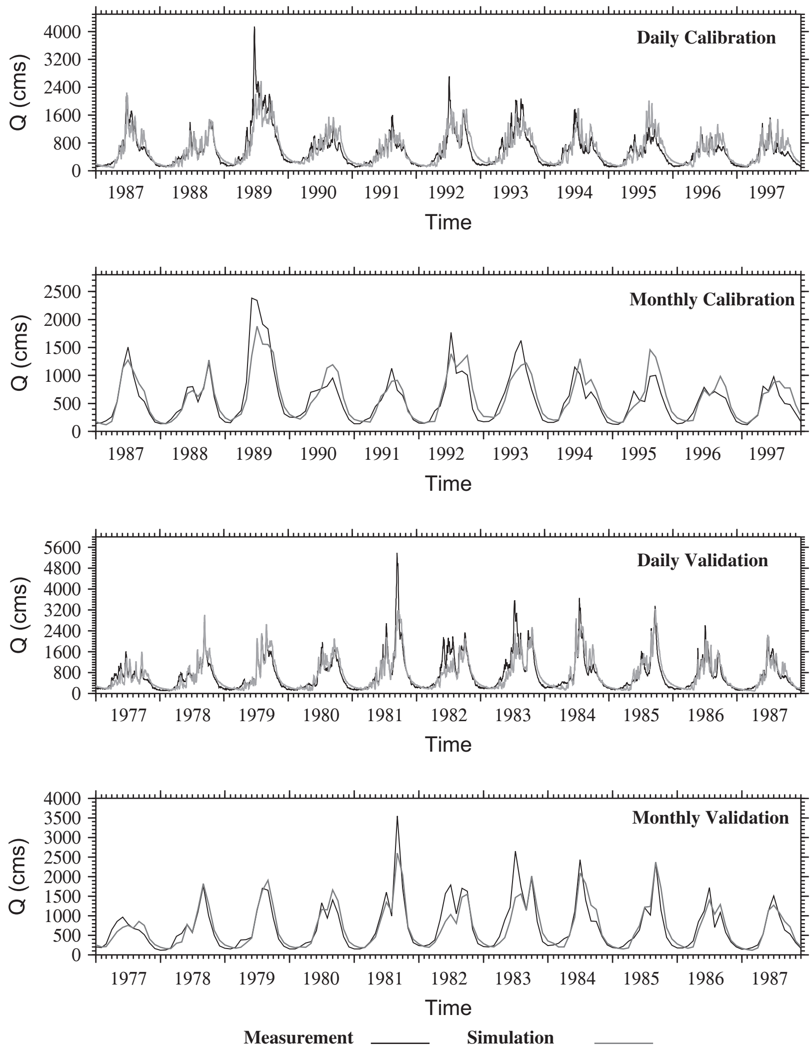

Fig. 4. Simulated and observed daily and monthly streamflow at TNH during the calibration period 1987–1997 and the validation period 1977–1987.

simulated annual snow cover over the short overlapping period was evident. EASE-Grid annual snow cover exhibited noticeable underestimation when compared to MODIS estimation and VIC simulation. Caution had to be taken when interpreting mean monthly snow cover because a different time period was used for EASE-Grid estimation. However, Fig. 5 demonstrates that VIC simulations satisfactorily captured seasonal cycles as satellite estimations. Overestimation was detected in VIC for January, February, November, and December when compared to MODIS measurements. During warmer months (May to September), VIC simulated snow cover was smaller than MODIS estimations but matched EASE-Grid snow data reasonably well. Differences between model simulated and satellite estimated monthly snow cover did not exceed 15% for any given month. Nevertheless, it was understood that both satellite estimations and VIC simulations contained large uncertainties concerning snow cover, making further improvements to the approach necessary.

The above analyses suggest that in general VIC performance was reasonable in resolving observed UYRB streamflow and snow cover. The following sections will use VIC to explore possible mechanisms behind observed streamflow changes.

6.3. Climate change

Fig. 6 shows annual precipitation, annual mean temperature (average of maximum and minimum temperature), and wind speed for the historical period (1957–2009), climate 1957, and climate 2009 for the area above JYR. The figure reveals that linear trends occurred in annual mean temperature for the historical period. Annual precipitation has large inter-annual variability. On average, precipitation increased by approximately 20 mm for climate 2009 compared to climate 1957. Annual mean temperature rose by approximately 1.6 °C for climate 2009 compared to climate 1957. Wind speed exhibited an abrupt change around 1969 (owing to the extensive anemometer upgrade that took place across China at that time). It decreased nearly linearly after 1969. Wind speed on average decreased by 0.3 m s^{-1} for climate 2009 compared to climate 1957. *F*-tests showed that trends in spatially averaged annual mean temperature and wind speed were statistically significant at $\alpha = 0.05$. Fig. 6 demonstrates that the inter-annual variability in the historical climate records were preserved for all three variables in climate 1957 and 2009. It also shows that temperature and wind speed in climate 1957 and climate 2009 well represented the beginning and ending status of the gradual climate change from 1957 to 2009.

In order to examine the effect of abrupt wind speed change around 1969, an adjusted wind speed time series was constructed by adding the monthly averaged differences between pre-1969 and 1969–1970 to the daily pre-1969 wind speed. The linear monthly trends that existed in 1957–1968 wind speed were remained in the adjusted time series. Post-1969 wind speed data were not changed.

Table 2
Statistics in the calibration and validation periods.

	Observation mean ($m^3\,s^{-1}$)	Simulation mean ($m^3\,s^{-1}$)	Bias (%)	*R*	RMSE ($m^3\,s^{-1}$)	Nash–Sutcliffe number
TNH	*Calibration (1987–1997)*					
Daily	576.2	601.2	4	0.86	246.1	0.74
Monthly	574.1	599.1	4	0.90	193.3	0.81
	Validation (1977–1987)					
Daily	714.1	708.7	−1	0.89	295.5	0.80
Monthly	711.4	706.1	−1	0.92	234.8	0.85
JMA	*Evaluation period 1 (1991–2000)*					
Daily	107.9	126.4	17	0.68	82.8	0.41
Monthly	107.5	126.1	17	0.74	69.5	0.49
	Evaluation period 2 (2001–2009)					
Daily	125.7	140.9	12	0.74	89.7	0.48
Monthly	125.2	140.4	12	0.78	78.0	0.55
TAK	*Evaluation period 1 (1987–1997)*					
Daily	61.0	45.3	26	0.84	43.11	0.57
Monthly	60.8	45.2	26	0.90	33.6	0.60
	Evaluation period 2 (1998–2009)					
Daily	53.6	41.4	22	0.77	34.2	0.53
Monthly	53.5	41.3	22	0.86	25.7	0.64
MAQ	*Evaluation period 1 (1987–1997)*					
Daily	414.2	428.7	4	0.87	300.7	0.76
Monthly	412.6	427.4	4	0.91	139.9	0.82
	Evaluation period 2 (1977–1986)					
Daily	514.3	529.3	3	0.88	237.5	0.77
Monthly	512.4	527.6	3	0.91	184.2	0.83

Note: *R* refers to correlation coefficient. RMSE refers to root mean square error.

Table 3
Calibrated and validated parameters and their values.

Parameters	Physical meaning	Values
bi	Variable infiltration curve parameter	0.023
Ds	Fraction of Dsmax where non-linear baseflow begins	0.646
Dsmax	Maximum velocity of baseflow	12.892
Ws	Fraction of maximum soil moisture where non-linear baseflow occurs	0.061
Exp	Exponent $n = 3 + 2$/lambda in Campbell's equation for hydraulic conductivity, where lambda = soil pore size distribution parameter	4.087
*D*1 (units: m)	Thickness of the first soil moisture layer	0.1
*D*2 (units: m)	Thickness of the second soil moisture layer	1.79
*D*3 (units: m)	Thickness of the third soil moisture layer	1.15

VIC simulations driven by the constructed and original wind speed time series were compared and the differences in water balance terms were computed. Results indicated that among the various water balance terms, only ET was affected the most but the differences in ET were less than 8 mm in annual averages for all sub-basins. Monthly averaged water balance terms were hardly affected by the adjustment due to the short record of 1957–1969 compared to 1969–2009. We concluded that the wind speed abrupt change around 1969 had negligible effects on the simulated annual and seasonal water balances and thus the original wind speed was used in subsequent analysis.

6.4. Response to climate variable changes

In order to understand the climate change impacts, it is necessary to investigate how water balance terms in sub-basins respond to changes in temperature, precipitation and wind speed separately as shown in Fig. 6. Table 4 presents the relative changes in water balance terms after temperature, precipitation and wind speed were perturbed. It is clear that increased temperature reduced available water resources and increased ET consumption (Table 4), consistent with the findings by Yang et al. (2011) who reported that increased ET corresponded to increased temperature over the Tibetan Plateau in recent decades. On the other hand, increased precipitation and decreased wind speed resulted in more available water. Table 4 also revealed that over the UYRB temperature changes impacted water balance terms the most, followed by precipitation changes and lastly by wind speed changes. Among the sub-basins, the impacts from temperature increase appeared to be more or less uniform especially for baseflow and ET; while precipitation changes affected water balance more for JMA than for other sub-basins, due to spatially varying precipitation changes as reported by Cuo et al. (2013).

6.5. Climate change impacts

Simulated differences in water balance terms between climate 2009 and climate 1957 for JMA, TAK, MAQ, TNH and LZH are provided in Fig. 7. Because of the short observation period at TAK (1981–2009), JMA, MAQ, TNH and LZH were focused on to determine the relationships between streamflow and water balance term changes. Terms examined included annual and monthly precipitation, ET, total surface runoff (runoff hereafter), baseflow, snowmelt runoff, and rainfall runoff. Except for TAK, all other basins exhibited increasing annual precipitation from 1957 to 2009, with JMA showing the largest increase (left panels in Fig. 7). All basins showed increasing annual ET but decreasing annual runoff, annual baseflow, and annual rainfall runoff except for JMA. Reductions in annual baseflow were slightly larger than those in annual runoff for TAK, MAQ, and TNH. Annual snowmelt runoff exhibited negligible changes for all basins, giving rise to nearly identical changes in runoff and rainfall runoff. This indicates that UYRB rainfall runoff dominates changes in annual totalsurface runoff. ET changes far exceeded precipitation changes for MAQ, TNH, and LZH, which, together with small decreases in runoff and baseflow, could explain large decreases in observed annual streamflow for MAQ, TNH and LZH (Fig. 2). For JMA, on the other hand, large increases in ET and precipitation virtually canceled

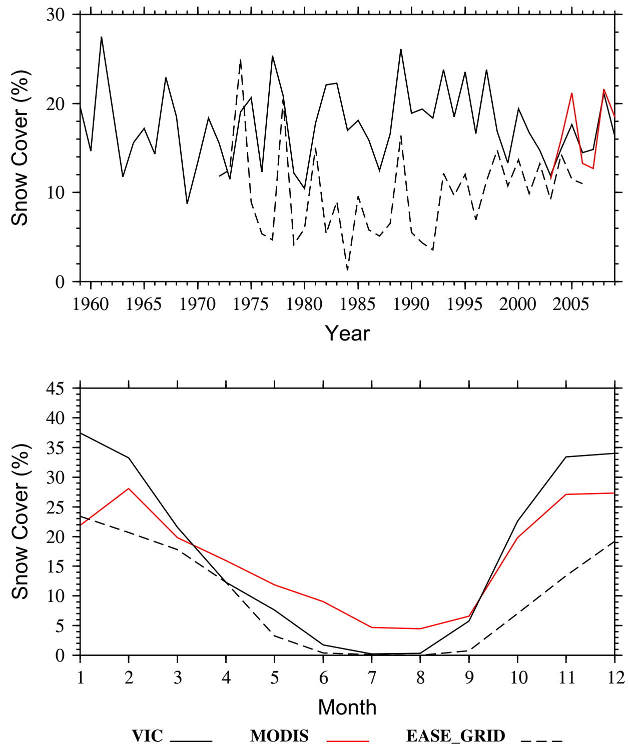

Fig. 5. Annual snow cover (%, upper panel) and seasonal snow cover (%, bottom panel) based on the VIC simulations (1959–2009 for upper panel and 2003–2009 for lower panel), MODIS estimation (2003–2009) and EASE-Grid estimation (1972–2006).

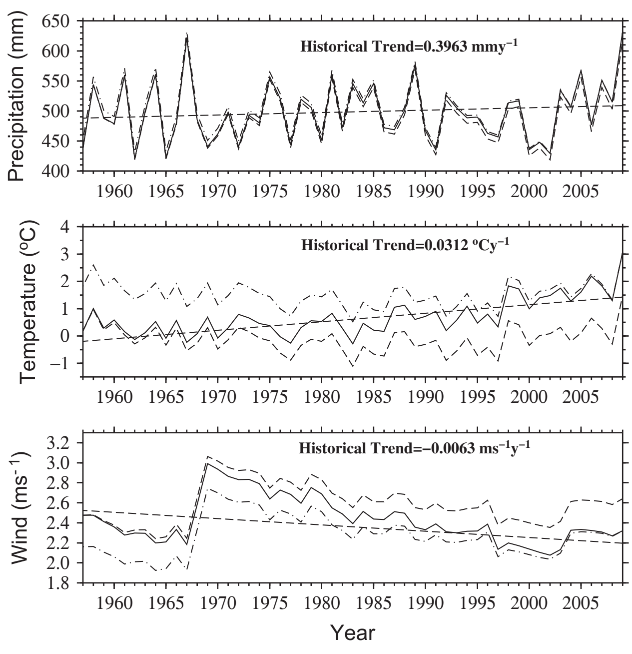

Fig. 6. Annual precipitation (mm), temperature (°C) and wind speed (m s^{-1}) for the historical period 1957–2009, climate 1957 and climate 2009 in the upper Yellow River Basin above JYR. Also shown are the linear trends for the historical period. Based on the *F*-test, trends in temperature and wind speed are statistically significant at 0.05 significance level.

each other out, which is likely responsible for the small changes observed in annual streamflow for JMA (Fig. 2).

Seasonally, water balance changes in the wet and warm season (May–September) dominated over those in the dry and cold season (October–April, right panels in Fig. 7). Precipitation notably decreased between July and September after small increasing in the first half of the year (from January to June) for MAQ, TNH, and LZH (Fig. 7). For all basins, May through November corresponded to high ET. Runoff and rainfall runoff (identical in both magnitude and pattern for all seasons) exhibited decreasing trends between July and September for TAK, MAQ, TNH, and LZH, which were consistent with changes in precipitation. For JMA, changes in runoff and rainfall runoff virtually amounted to null. Little change was detected for seasonal snowmelt runoff between climate 2009 and climate 1957 indicating that the contribution of snow to streamflow change in the UYRB was small, differing from the Puget Sound basin situated in the PNW of the United States of America. Baseflow increased slightly in May and June and then decreased in the second half of the year with peaks occurring in September or October for all sub-basins. Such changes in baseflow and precipitation may explain the forward movement of the day representing the midpoint of yearly mass flow as it was identified in observed streamflow (see Fig. 3). As a further demonstration of this effect, the simulated VIC midpoint day of yearly mass flow occurred 7, 8, 8, 6, and 5 days earlier for climate 2009 than for climate 1957 at JMA, TAK, MAQ, TNH and LZH, respectively.

When comparing Figs. 2–7, it becomes clear that the large decreases in observed streamflow for JMA, MAQ and TNH that occurred between July and September were the result of increased ET and reduced precipitation. For June, statistically insignificant increases for JMA, MAQ, and TNH (Fig. 2) were likely due to increased precipitation (Fig. 7).

In January–May, observed streamflow exhibited negligible increases for JMA, but relatively large decreases for MAQ and TNH due to the change in baseflow (Figs. 2 and 7). For LZH, precipitation changes nearly canceled out ET changes in January–May (Fig. 7), whereas observed streamflow still showed significant increases during the same time period (Fig. 2).

In October, precipitation fell as snow in the most part of the UYRB and it offered little contribution to overall streamflow. On the other hand, increased ET in October reduced baseflow, hence reducing streamflow. November saw slight decreases (increases) in precipitation (ET) in all basins while little change in precipitation and ET was seen in December (Fig. 7). Consequently, observed streamflow for all sub-basins except LZH showed slight decreases in November and virtually no changes in December (Fig. 2). For TAK, VIC simulated changes in water balance terms could also explain the observed trends rather well (Figs. 2 and 7). Unlike the other sub-basins, observed streamflow trends for LZH could not be accounted for by climate change impacts alone, indicating that land cover/use change and reservoir operations play important roles for LZH.

6.6. Land cover change impacts

Observed and simulated annual streamflow using historical climate records and land cover 1960s is shown in Fig. 8 for JMA, MAQ, TNH and LZH. The similarity between observed and simulated streamflow for JMA, MAQ and TNH, and large differences for LZH indicated that land cover/use change impacts were small above TNH but large for LZH. Differences in land cover/use change impacts above and below TNH were likely related to differences in population density: low density above TNH but much high density below TNH. High population density indicates intense water use activity related to agriculture, industry and municipality. The differences between the simulations and observations at LZH were large even in the 1960s implying that human activity had altered streamflow even before the 1960s.

Table 4
Relative changes in water balance terms in all sub-basins due to changes in temperature, precipitation and wind speed. *T*: temperature, *P*: precipitation, *W*: wind speed, RF: runoff, ET: evapotranspiration.

Basins	Water balances	Climate 1957 (mm)	*T*change (%)	*P*change (%)	*W* change (%)
JMA	Baseflow	86.3	−36	24	3
	ET	311.0	11	6	−1
	Precipitation	412.2	0	11	0
	Surface RF	14.6	−18	19	6
	RF_rainfall	12.4	−14	19	5
	RF_snowmelt	2.1	−49	21	14
TAK	Baseflow	111.9	−28	8	2
	ET	433.9	11	1	−1
	Precipitation	805.0	0	3	0
	Surface RF	257.8	−7	5	2
	RF_rainfall	228.9	−4	3	1
	RF_snowmelt	28.9	−26	16	7
MAQ	Baseflow	115.8	−32	17	3
	ET	362.5	12	3	−1
	Precipitation	561.2	0	5	0
	RF	82.6	−8	2	2
	RF_rainfall	73.3	−5	0	1
	RF_snowmelt	9.3	−30	13	7
TNH	Baseflow	100.7	−33	14	3
	ET	348.2	12	4	−2
	Precipitation	538.4	0	6	0
	RF	89.0	−9	3	3
	RF_rainfall	78.8	−6	2	2
	RF_snowmelt	10.2	−31	13	9
LZH	Baseflow	55.8	−32	17	5
	ET	292.4	11	5	−1
	Precipitation	494.1	0	5	0
	RF	145.0	−9	2	2
	RF_rainfall	130.6	−6	0	1
	RF_snowmelt	14.4	−33	12	9

Differences between the simulations and observations started to amplify for JMA, MAQ, TNH and LZH after 1980 (Fig. 8) when the economy started to boost. Since the 1980s, streamflow has been increasingly withdrawn for agriculture, industry, and municipal water use. For example, about 70% of the total water supply ($36.6 \times 10^8\ m^3$) in Qinghai Province was surface water in 2011 (Qinghai Water Resources Bulletin, 2011). Out of the total water supply, 67% was used for agricultural practices, 25% for industry and 7% for urban activity in 2011 (Qinghai Water Resources Bulletin, 2011). In Gansu Province, in the Yellow River Basin above (and including) Lanzhou City, about 85% of the total water supply ($10.31 \times 10^8\ m^3$) came from surface water in 2010 (Yearbook of Gansu Water Resources, 2011). Out of the total water supply, 50% was used for agriculture, 35% for industry and 10% for urban activity (Yearbook of Gansu Water Resources, 2011). Due to data limitation, we were not able to investigate the temporal changes of water supply and water usage for this region. Nevertheless, the statistics in 2011 and 2010 for Qinghai and Gansu provinces clearly showed that human activity had greatly affected streamflow.

Differences between observed and simulated streamflow after 2000 when the conservation projects were implemented were visually similar to those in the 1980s and 1990s for JMA, MAQ and TNH (Fig. 8), indicating that the conservation projects have yet to exert significant influences on annual streamflow. Simulations using land cover 1994 and historical climate records produced nearly identical results (not shown).

Trends of monthly streamflow residual (observation minus simulation) describe land cover change impacts over the past decades. A positive (negative) residual trend suggests positive (negative) land cover change impacts, as the observations and simulations both experience the same climate change if assuming a linear climate and land cover/use change relation.

Fig. 9 presents the trends in residual for 1957–2009 (top four panels,) and 1994–2009 (bottom four panels), representing the long-term and recent land cover/use change impacts, respectively. Over the long-term, residual had been mostly decreasing in the warm season, indicating negative impacts of land cover change on streamflow. In the cold season for JMA, MAQ and TNH, residual had been mostly increasing from October through December but decreasing from January through April. It seemed that land cover/use change impacts were similar to climate change impacts in the warm season by reducing streamflow for JMA, MAQ and TNH. For LZH, the trends were always the largest amongst the sub-basins and consistency was noted between residual trends (Fig. 9) and observed trends (Fig. 2) for both the monthly and annual time scales, further illustrating the important impacts of land cover/use change for this sub-basin.

Differences were noted between the long-term and recent land cover/use change impacts (Fig. 9), with more positive monthly and annual trends after 1994. This indicates that the GGP and TRSRR may have started to exert some positive effects on water resources in the region, although a longer time may be needed for the effects to fully emerge and become significant.

As for the reservoir impact on streamflow, our analysis showed that due to the existence of Longyang Gorge and Liujia Gorge, mean annual flow below the dams were reduced by only 3% and 2%, respectively, indicating a minimal impact of the dams on mean annual flow. However, the dams did alter the seasonalflow distributions as shown in Fig. 10. At both dams, outflow was greater than inflow in January–May and November–December, while outflow was smaller than inflow in June–October, suggesting that negative streamflow trends in June–October and positive trends in December–May for LZH could also be partly explained by the reservoir operations. Notice that the differences between outflow and inflow were larger for Longyang Gorge than for Liujia Gorge (Fig. 10).

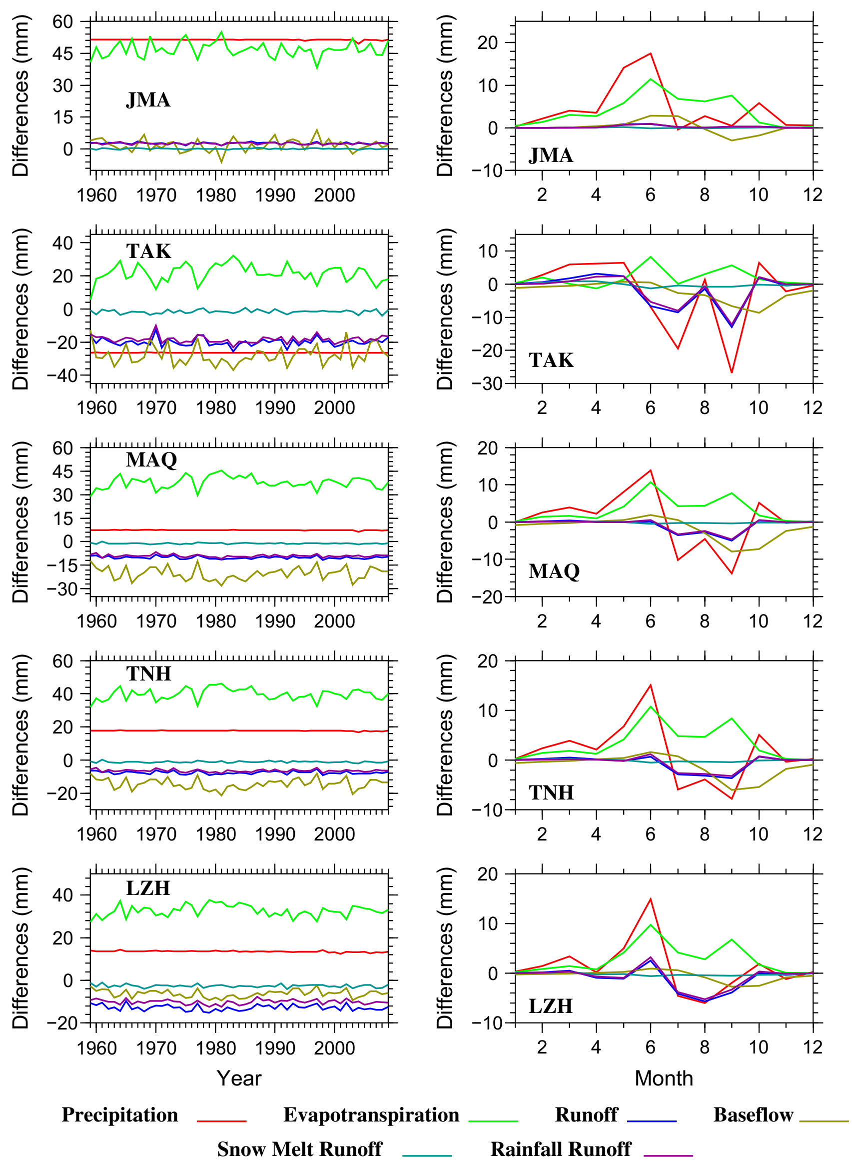

Fig. 7. VIC simulated annual differences (left panels) and seasonal differences (right panels) in water balance terms between climate 2009 and 1957 for five sub-basins (JMA, TAK, MAQ, TNH and LZH).

7. Discussions

7.1. Model uncertainty

Model uncertainty resulted from uncertainties in input data, model dynamics and physics, and parameter values is one of the reasons that hydrological models need to be calibrated and validated. To examine the suitability of the VIC model for impact studies in the UYRB, the model was calibrated and validated at four gauges in the headwater region that were not affected by major dams or significant flow diversions. The calibration and validation results showed that VIC simulations matched observations well in various periods at all gauges (Fig. 4 and Table 2). While this ensures that the VIC model is applicable in the region, it is recognized that VIC showed relatively large biases in terms of peak flows that were most likely due to errors in extreme precipitation in the forcing data. The model biases in peak flows, however, should not compromise our analysis results in any significant way since the analysis was not focused on extremes. Another area of concern is snow. As mentioned before, both observations and simulations seemed to contain large uncertainties in terms of snow cover. While it is difficult to assess the magnitude of model biases in snow cover, consistency in streamflow between simulations and observations suggests that the VIC simulated snow was reasonable.

7.2. Snow contribution

Simulations using historical forcing records showed that in November–April, streamflow was dominated by baseflow. In March and April (May) for TAK, MAQ, TNH and JYR (JMA), snow melt runoff was about 10–35% of the total month streamflow, which only accounted for about 5–13% of the total annual streamflow in the respective sub-basins. This is largely consistent with the findings by Lan et al. (1999) who showed that during late March–early June snow melt contributed less than 40% of the streamflow for TNH, and also corroborated Immerzeel et al. (2010)'s results with an extended time period. Thus, snow melt contribution seems to be important only during the melting season before the onset of the raining season when baseflow still

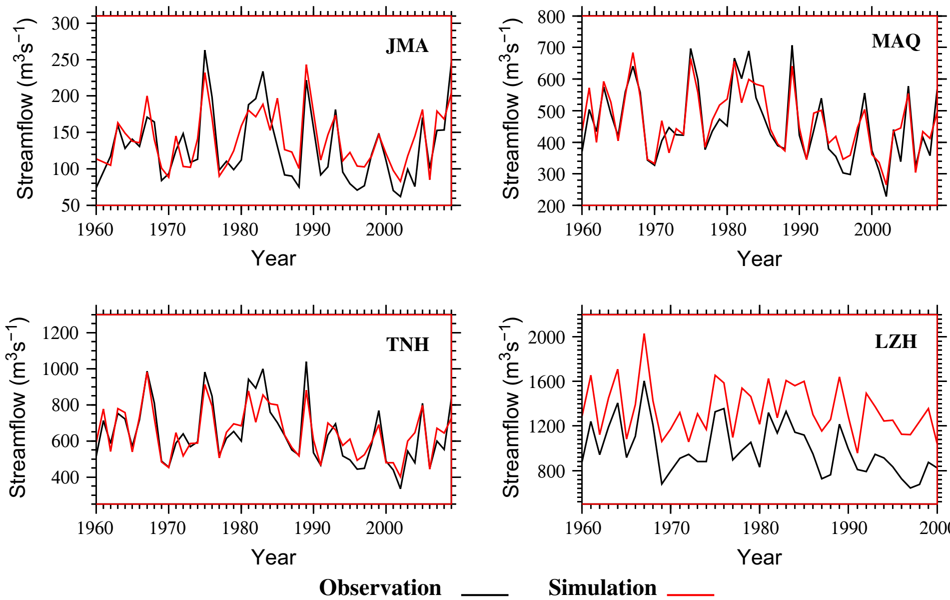

Fig. 8. Observed annual streamflow and VIC simulated annual streamflow using land cover 1960s for four sub-basins (JMA, MAQ, TNH, and LZH).

dominates. The major contributions to water resources in the UYRB appear to be rainfall runoff and baseflow.

The limited melt water contribution in this region is most likely due to the reasons as follow. First, roughly 85% of annual precipitation takes place during the wet and warm season when average air temperature is approximately 9 °C. Only 15% of annual precipitation is recorded in the dry and cold season. There are essentially no glacial in the UYRB (Immerzeel et al., 2010). Second, during the wet and warm season, only 5% precipitation falls as snow. Third, average air temperature remains −5 °C in the dry and cold season, which is much lower than 1.6 °C, the lower limit for rain to occur and 3.4 °C, the upper limit for snow to occur (Cuo et al., 2013). The limited contribution by snow melt can also be explained by the elevation–area relationship (Casola et al., 2009). According to Lan et al. (1999), in late April, snow covers areas with elevation above 4000 m, and average snow line is about 5000 m in the UYRB. Hypsometric analysis based on 1-km elevation map shows that about 34% of area in the UYRB has elevation above 4000 m, but areas with elevation greater than 5000 m are less than 1%. We argue that on top of the limited snowfall, areas to keep snow are also limited in the UYRB.

7.3. Relationship between hydrology and the cryospheric changes

Besides snow, vast areas of permafrost and seasonally frozen ground (SFG), two of the major components of the cryosphere, exist over the TP (Zhou and Guo, 1982; Zhou et al., 2000; Cheng and Jin, 2013). The presence of permafrost and SFG limits moisture exchanges among the surface, the frozen layer(s), and the underlying unfrozen soils, and reduces soil surface infiltration capacity and soil hydraulic conductivity, alters land surface flow, ground water transportation and affects ecosystem (Cherkauer and Lettenmaier, 1999; Koren et al., 1999; Niu and Yang, 2006; Bense et al., 2012; Gouttevin et al., 2012; Cheng and Jin, 2013).

In recent decades, due to the combined influences of climate change and human activities, increasing permafrost temperature, permafrost degradation, rising active layer thickness above permafrost and decreasing duration of SFG have been observed over the TP (Zhao et al., 2004; Fu et al., 2007; Lemke et al., 2007; Cheng and Wu, 2007; Zhang, 2007; Wu and Zhang, 2008; Cheng and Jin, 2013). Impacts of permafrost degradation over the TP and its downstream areas include intensified exchange of heat between the atmosphere and the ground surface (Li et al., 2002), a dropping groundwater table at the source areas of the Yangtze River and Yellow River (Cheng and Wu, 2007), and changes in water resources (Cheng and Jin, 2013), with potentially far-reaching effects on the Asian monsoons and the carbon dioxide budget (Cheng and Wu, 2007; Zhang, 2007; Kang et al., 2010).

In the entire UYRB, discontinuous and sporadic permafrost and SFG are identified (Cheng and Jin, 2013). Like the rest of the TP, permafrost in the UYRB has been degrading in recent decades. Jin et al. (2011) showed that permafrost degrades more rapidly on eastern and northeastern margins of the TP where the UYRB is located when compared to the interior TP. Such accelerated degradation of permafrost in the UYRB would have profound effects on the hydrology (Jin et al., 2009, 2012), as summarized by Cheng and Jin (2013) as follows: (a) a negative water balance in local soil and lakes as a result of increased terrestrial evaporation and declined river runoff, and (b) diminishing water resources as evidenced by lowering water tables, shrinking lakes and wetlands, and frequent exposure of the Yellow River bed. It is unclear, however, to what extent permafrost degradation has caused changes in water resources in this region.

Largely consistent with what the aforementioned papers reported, this study finds diminishing streamflow in the UYRB in recent decades. Though this study attributes the changes in streamflow to the combined effects of changes in precipitation, ET, rainfall runoff, and baseflow caused primarily by climate change in the area above TNH, it is highly possible that permafrost degradation have played a role in those changes as well. As an example, when permafrost is thawed, it can be changed from an aquitard to an aquifer in some areas and talik channels can be formed or enlarged, which facilitate surface water infiltration, subsurface flow increase and groundwater recharge (Cheng and Jin, 2013). To what degree permafrost degradation impacts hydrological processes and ecosystems in the UYRB deserves closer examinations and this will be the focus of our future study.

8. Conclusions

UYRB hydrological regimes have exhibited changes over the past decades as manifested by decreases in annual streamflow, a progressively greater overall streamflow during the early part of the year compared to the latter part, and the forward movement

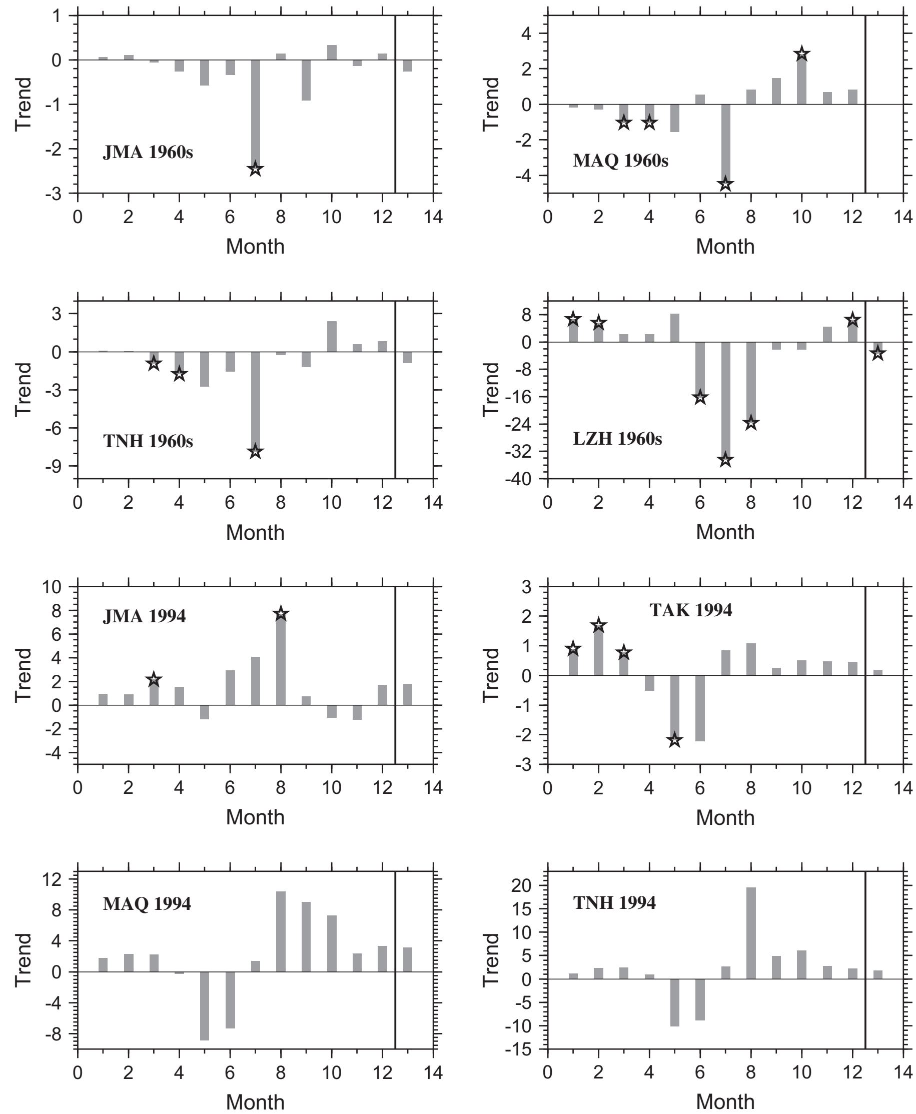

Fig. 9. Monthly and annual trends of residuals between observed and simulated streamflow for 1957–2009 (upper four panels) and 1994–2009 (bottom four panels). Simulations were conducted using land cover 1960s (top four panels) and land cover 1994 (bottom four panels) to show long-term and recent land cover change impacts. Stars represent trends that are statistically significant at 0.10 significance level.

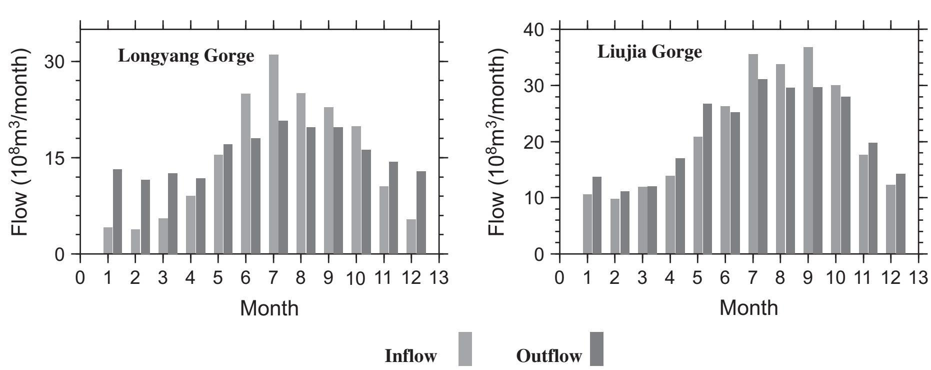

Fig. 10. Mean monthly inflow and outflow of Longyang Gorge (1986–2002) and Liujia Gorge (1968–2002).

of the day representing the midpoint of yearly mass flow. These changes in observed streamflow were determined to be combined effects of changes in precipitation, ET, rainfall runoff, and baseflow caused primarily by climate change in the area above TNH. Snow-melt runoff playsa modest role in UYRB hydrology. Below TNH where human activity is relative intense, the impacts of land cover change/use including agriculture, industry, urbanization, and reservoir operations become important. The GGP and TRSRR conservation programs have started to show positive effects on water resources in the UYRB.

Acknowledgements

This study was supported by the National Basic Research Program (Grant No. 2013CB956004), the National Basic Research Program of China (Grant No. 2010CB951101), and by the Hundred Talent Program granted to Lan Cuo by the Chinese Academy of Sciences. Qiuhong Tang generously provided daily streamflow data at LZH station.

References

Abdulla, F.A., Lettenmaier, D.P., 1997. Development of regional parameter estimation equations for a macroscale hydrologic model. Journal of Hydrology 197, 230–257.

Adam, J.C., Haddeland, I., Su, F., Lettenmaier, D.P., 2007. Simulation of reservoir influences on annual and seasonal streamflow changes for the Lena Yenisei, and Ob' rivers. Journal Geophysical Research 112 (D2411). http://dx.doi.org/10.1029/2007JD008525.

Armstrong, R.L., Brodzik, M.J., 2005. Northern Hemisphere EASE-Grid Weekly Snow Cover and Sea Ice Extent Version 3. Boulder, Colorado USA: National Snow and Ice Data Center. Digital Media.

Barnett, T., Adam, J.C., Lettenmaier, D.P., 2005. Potential impacts of a warming climate on water availability in snow-dominated regions. Nature 438, 303–309. http://dx.doi.org/10.1038/nature04141.

Bense, V.F., Kooi, H., Ferguson, G., Read, T., 2012. Permafrost degradation as a control on hydrogeological regime shifts in a warming climate. Journal of Geophysical Research 117, F03036. http://dx.doi.org/10.1029/2011JF002143.

Bowling, L.C., Storck, P., Lettenmaier, D.P., 2000. Hydrologic effects of logging in western Washington, USA. Water Resources Research 36 (11), 3223–3240.

Cai, X., Rosegrant, M.W., 2004. Optional water development strategies for the Yellow River Basin: balancing agricultural and ecological water demands. Water Resources Research 40, W08S04. http://dx.doi.org/10.1029/2003WR002488.

Cao, J., Qin, D., Kang, E., Li, Y., 2006. River discharge changes in the Qinghai-Tibet Plateau. Chinese Science Bulletin 51 (5), 594–600. http://dx.doi.org/10.1007/s11434-006-0594-6.

Casola, J.H., Cuo, L., Livneh, B., Lettenmaier, D.P., Mote, P.W., Wallace, J.M., 2009. Assessing the impacts of global warming on snowpack of the Washington cascades. Journal of Climate 22, 2758–2772. http://dx.doi.org/10.1175/2008JCLI2612.1.

Chen, L.Q., Liu, C.M., 2007. Influence of climate and land cover change on runoff of the source regions of Yellow River. China Environmental Science 27 (4), 559–565 (in Chinese).

Cheng, G., Jin, H., 2013. Permafrost and groundwater on the Qinghai-Tibet Plateau and in northeast China. Hydrogeology Journal 21, 5–23.

Cheng, G., Wu, T., 2007. Responses of permafrost to climate change and their environmental significance, Qinghai-Tibet Plateau. Journal of Geophysical Research 112, F02S03. http://dx.doi.org/10.1029/2006JF000631.

Cherkauer, K.A., Lettenmaier, D.P., 1999. Hydrological effects of frozen soils in the upper Mississippi River basin. Journal of Geophysical Research 104 (D16), 19599–19610.

Cherkauer, K.A., Lettenmaier, D.P., 2003. Simulation of spatial variability in snow and frozen soil. Journal of Geophysical Research 108 (D22), 8858. http://dx.doi.org/10.1029/2003JD003575.

Christensen, N.S., Wood, A.W., Voisin, N., Lettenmaier, D.P., Palmer, R.N., 2004. The effects of climate change on the hydrology and water resources of the Colorado River Basin. Climatic Change 62, 337–363. http://dx.doi.org/10.1023/B:CLIM.0000013684.13621.1f.

Cuo, L., Lettenmaier, D.P., Marina, A., Richey, J.E., 2009. Effects of a century of land cover and climate change on the hydrology of the Puget Sound basin. Hydrological Processes 6, 907–933. http://dx.doi.org/10.1002/hyp.7228.

Cuo, L., Beyene, T.K., Voisin, N., Su, F., Lettenmaier, D.P., Alberti, M., Richey, J.E., 2011. Effects of mid-twenty-first century climate and land cover change on the hydrology of the Puget Sound basin, Washington. Hydrological Processes 25 (11), 1729–1735. http://dx.doi.org/10.1002/hyp.7932.

Cuo, L., Zhang, Y., Wang, Q., Zhang, L., Zhou, B., Hao, Z., Su, F., 2013. Climate change in the northern Tibetan Plateau during 1957–2009: spatial patterns and possible mechanisms. Journal of Climate 26, 85–109. http://dx.doi.org/10.1175/JCLI-D-11-00738.1.

Dong, L., Wang, W., Kong, J., Shi, H., Guo, Z., Mai, L., 2005. Supervise of eco-environmental change based on RS methods and causal analysis in Maduo County in upriver regions of the Yellow River. Bulletin of Soil and Water Conservation 25 (4), 68–72 (in Chinese).

Durre, I., Wallace, J.M., Lettenmaier, D.P., 2000. Dependence of extreme daily maximum temperature on antecedent soil moisture in the contiguous United States during summer. Journal of Climate 13, 2641–2651.

FAO/IIASA/ISRIC/ISS-CAS/JRC, 2008. Harmonized World Soil Database (version 1.0). FAO, Rome, Italy and IIASA, Laxenburg, Austria.

Fu, G.B., Chen, S.L., Liu, C.M., Shepard, D., 2004. Hydro-climatic trends of the Yellow River basin for the last 50 years. Climatic Change 65, 149–178. http://dx.doi.org/10.1023/B:CLIM.0000037491.95395.bb.

Fu, Y., Li, F., Zhang, G., Yang, Q., Zeng, X., 2007. Natural grasslands degradation and environmental driving factors in Qinghai Province. Journal of Glaciology and Geocryology 29 (4), 525–535 (in Chinese).

Gao, Y., Vano, J.A., Zhu, C., Lettenmaier, D.P., 2011. Evaluating climate change over the Colorado River basin using regional climate models. Journal of Geophysical Research 116, D13104. http://dx.doi.org/10.1029/2010JD015278.

Gouttevin, I., Krinner, G., Ciais, P., Polcher, J., Legout, C., 2012. Multi-scale validation of a new freezing scheme for a land-surface model with physically-based hydrology. The Cryosphere 6, 407–430. http://dx.doi.org/10.5194/tc-6-407-2012.

Haddeland, I., Lettenmaier, D.P., Skaugen, T., 2006. Effects of irrigation on the water and energy balances of the Colorado and Mekong river basins. Journal of Hydrology 324, 210–223. http://dx.doi.org/10.1016/j.jhydrol.2005.09.028.

Hamlet, A., Mote, P.W., Clark, M.P., Lettenmaier, D.P., 2005. Effects of temperature and precipitation variability on snowpack trends in the western United States. Journal of Climate 18, 4545–4561. http://dx.doi.org/10.1175/JCLI3538.1.

Hansen, M., DeFries, R., Townshend, J.R.G., Sohlberg, R., 2000. Global land cover classification at 1 km resolution using a decision tree classifier. International Journal of Remote Sensing 21, 1331–1365.

Hu, Y., Maskey, S., Uhlenbrook, S., Zhao, H., 2011. Streamflow trends and climate linkages in the source region of the Yellow River, China. Hydrological Processes. http://dx.doi.org/10.1002/hyp.8069.

Huang, Y., Cai, J., Yin, H., Cai, M., 2009. Correlation of precipitation to temperature variation in the Huanghe River (Yellow River) basin during 1957–2006. Journal of Hydrology 372, 1–8. http://dx.doi.org/10.1016/j.jhydrol.2009.03.029.

Immerzeel, W.W., van Beek, L.P.H., Bierkens, M.F.P., 2010. Climate change will affect the Asian water towers. Science 328, 1382–1385. http://dx.doi.org/10.1126/science.1183188.

Jin, H.J., He, R.X., Cheng, G.D., Wu, Q.B., Wang, S.L., Lü, L.Z., Chang, X.L., 2009. Changes in frozen ground in the Source Area of the Yellow River on the Qinghai-Tibet Plateau, China, their eco-environmental impacts. Environmental Research Letters 4 (4). http://dx.doi.org/10.1088/1748-9326/4/4/045206.

Jin, H.J., Luo, D.L., Wang, S.L., Lü, L.Z., Wu, J.C., 2011. Spatiotemporal variability of permafrost degradation on the Qinghai-Tibet Plateau. Sciences in Cold and Arid Regions 3 (4), 281–305.

Jin, H.J., Cheng, G.D., Wu, Q.B., Wang, S.L., Luo, D.L., Marchenko, S.S., 2012. Degradation of permafrost in the source areas of the Yellow River on the northeastern Qinghai-Tibet Plateau and its ecological and hydro(geo)logical impacts: status, issues, and prospects. In: Ma, W., Niu, F.J. (Eds.), Research Monograph of Cold and Arid Regions Engineering and Environment: A Collection of the Papers Dedicated to the 70th Birthday of Academician Guodong Cheng. Lanzhou University Press, Lanzhou, pp. 229–239 (in Chinese).

Kang, S., Wu, Y., You, O., Flügel, W.-A., Pepin, N., Yao, T., 2010. Review of climate and cryospheric change in the Tibetan Plateau. Environmental Research Letters 5. http://dx.doi.org/10.1088/1748-9326/5/1/015101.

Koren, V., Schaake, J., Mitchell, K., Duan, Q.-Y., Chen, F., Baker, J.M., 1999. A parameterization of snowpack and frozen ground intended for NCEP weather and climate models. Journal of Geophysical Research 104 (D16), 19569–19585.

Lan, Y., Kang, E., Ma, Q., Yang, W., Yao, Z., 1999. Runoff forecast model for inflow to the Longyangxia reservoir in the upper Yellow River basin during spring. Journal of Glaciology and Geocryology 21 (4), 391–395.

Lemke, P., Ren, J., Alley, R.B., Allison, I., Carrasco, J., Flato, G., Fuji, Y., Kaser, G., Mote, P., Thomas, R.H., Zhang, T., 2007. Observations: changes in snow, ice and frozen ground. In: Solomon, S., Qin, D., Manning, M., Chen, Z., Marquis, M., Averyt, K.B., Tignor, M., Miller, H.L. (Eds.), Climate Change 2007: The Physical Science Basis. Contribution of Working Group I to the Fourth Assessment Report of the Intergovernment Panel on Climate Change. Cambridge University Press, Cambridge, United Kingdom.

Li, D., Liu, C., 2004. Study on land-cover change of the source regions of the Yellow River Basin in the past 10 years. Journal of Beijing Normal University (Natural Science) 40 (2), 269–275 (in Chinese).

Li, S., Nan, Z., Zhao, L., 2002. Impact of soil freezing and thawing process on thermal exchange between atmosphere and ground surface. Journal of Glaciology and Geocryology 24 (5), 506–511 (in Chinese with English abstract).

Liang, X., Lettenmaier, D.P., Wood, E.F., 1994. A simple hydrologically based model of land surface water and energy fluxes for general circulation models. Journal of Geophysical Research 99 (D7), 14415–14428.

Liang, X., Wood, E.F., Lettenmaier, D.P., 1996. Surface soil moisture parameterization of the VIC-2l model: evaluation and modification. Global and Planetary Change 13, 195–206.

Lohmann, D., Raschke, E., Nijssen, B., Lettenmaier, D.P., 1998a. Regional scale hydrology: I. Formulation of the VIC-2l model coupled to a routing model. Hydrological Sciences Journal 43 (1), 131–141.

Lohmann, D., Raschke, E., Nijssen, B., Lettenmaier, D.P., 1998b. Regional scale hydrology. II. Application of the VIC-2l model to the Weser River, Germany. Hydrological Sciences Journal 43 (1), 143–158.

Matheussen, B., Kirschbaum, R.L., Goodman, I.A., O'Donnel, G.M., Lettenmaier, D.P., 2000. Effects of land cover change on streamflow in the interior Columbia River Basin (USA and Canada). Hydrological Processes 14, 867–885.

Mote, P., Salathe Jr., E.P., 2010. Future climate in the Pacific Northwest. Climatic Change 102, 29–50. http://dx.doi.org/10.1007/s10584-010-9848-z.

Nijssen, B., Schnur, R., Lettenmaier, D.P., 2001. Global retrospective estimation of soil moisture using the Variable Infiltration Capacity land surface model, 1980–1993. Journal of Climate 14, 1790–1808.
Niu, G.-Y., Yang, Z.-L., 2006. Effects of frozen soil on snowmelt runoff and soil water storage at a continental scale. Journal of Hydrometeorology 7, 937–952.
Qinghai Water Resources Bureau, 2011. Qinghai Water Resources Bulletin 2011 (in Chinese).
Rhoads, J., Dubayah, R., Lettenmaier, D., O'Donnel, G., Lakshmi, V., 2001. Validation of land surface models using satellite-derived surface temperature. Journal of Geophysical Research 106 (D17), 20085–20099.
Rodriguez-Iturbe, I., Porporato, A., Laio, F., 2001. Intensive or extensive use of soil moisture: plant strategies to cope with stochastic water availability. Geophysical Research Letters 28 (23), 4495–4497. http://dx.doi.org/10.1029/2001GL012905.
Shepard, D.S., 1984. Computer mapping: the SYMAP interpolation algorithm. In: Gaile, Willmott (Ed.), Spatial Statistics and Models. Reidel Publishing Company, Hingham, MA, USA.
Stewart, I.T., 2009. Changes in snowpack and snowmelt runoff for key mountain regions. Hydrological Processes 23, 78–94. http://dx.doi.org/10.1002/hyp.7128.
Stewart, I.T., Cayan, D.R., Dettinger, M.D., 2005. Changes toward earlier streamflow timing across western north America. Journal of Climate 18, 1136–1155.
Tang, Q., Oki, T., Kanae, S., Hu, H., 2008. Hydrological cycles change in the Yellow River Basin during the last half of the twentieth century. Journal of Climate 21, 1790–1806. http://dx.doi.org/10.1175/2007JCLI1854.1.
Todini, E., 1996. The ARNO rainfall–runoff model. Journal of Hydrology 175, 339–382.
Wang, G., Qian, J., Cheng, G., Lai, Y., 2001. Eco-environmental degradation and causal analysis in the source region of the Yellow River. Environmental Geology 40, 884–890.
Wu, Q., Zhang, T., 2008. Recent permafrost warming on the Qinghai-Tibetan Plateau. Journal of Geophysical Research 113, D13108. http://dx.doi.org/10.1029/2007JD009539.
Xu, Z.X., Li, J.Y., Liu, C.M., 2007. Long-term trend analysis for major climate variables in the Yellow River Basin. Hydrological Processes 21, 1935–1948. http://dx.doi.org/10.1002/hyp.6405.
Yang, D., Li, C., Hu, H., Lei, Z., Yang, S., Kusuda, T., Koike, T., Musiake, K., 2004. Analysis of water resources variability in the Yellow River of China during the last half century using historic data. Water Resources Research 40, W06502. http://dx.doi.org/10.1029/2003WR002763.
Yang, K., Ye, B., Zhou, D., Wu, B., Foken, T., Qin, J., Zhou, Z., 2011. Response of hydrological cycle to recent climate changes in the Tibetan Plateau. Climatic Change 109, 517–534. http://dx.doi.org/10.1007/s10584-011-0099-4.
Yearbook of Gansu Water Resources, 2011. Yearbook of Gansu Water Resources Bulletin (in Chinese).
Zhang, T., 2007. Perspectives on environmental study of response to climatic and land cover/land use change over the Qinghai-Tibetan Plateau: an introduction. Arctic, Antarctic, and Alpine Research 39, 631–634.
Zhang, Q., Xu, C.Y., Zhang, Z., Ren, G., Chen, Y.D., 2008. Climate change or variability? The case of Yellow river as indicated by extreme maximum and minimum air temperature during 1960–2004. Theoretical Application of Climatology 93, 35–43.
Zhao, R.J., Zhang, Y.L., Fang, L.R., Liu, X.R., Zhang, Q.S., 1980. The Xinanjiang model. In: Hydrological Forecasting Proceedings, Oxford Symposium. IASH Publ., 129, pp. 351–356.
Zhao, L., Ping, C.-L., Yang, D., Cheng, G., Ding, Y., Liu, S., 2004. Changes of climate and seasonally frozen ground over the past 30 years in Qinghai-Xizang (Tibetan) Plateau, China. Global and Planetary Change 43, 19–31.
Zhao, F.F., Xu, Z.X., Huang, J.X., 2007. Long-term trend and abrupt change for major climate variables in the upper Yellow River Basin. Acta Meteorology Sinica 21 (2), 204–214.
Zhao, F., Xu, Z., Zhang, L., Zuo, D., 2009. Streamflow response to climate variability and human activities in the upper catchment of the Yellow River Basin. Science in China Series E: Technological Sciences 52 (11), 3249–3256. http://dx.doi.org/10.1007/s11431-009-0354-3.
Zheng, H., Zhang, L., Zhu, R., Liu, C., Sato, Y., Fukushima, Y., 2009. Response of streamflow to climate and land surface change in the headwaters of the Yellow River Basin. Water Resources Research 45, W00A19. http://dx.doi.org/10.1029/2007WR006665.
Zhou, Y.W., Guo, D.X., 1982. Principal characteristics of permafrost in China. Journal of Glaciology and Geocryology 4 (1), 1–19 (in Chinese).
Zhou, X., Wang, Z., Du, Q., 1987. Qing Hai Vegetation. Qing Hai Ren Ming Publisher, Xi Ning, Qing Hai, China (in Chinese).
Zhou, Y.W., Qiu, G.Q., Guo, D.X., Li, S.D., 2000. Frozen Ground in China. Science Press, Beijing, pp. 128–136 (in Chinese).